PLASU Journal of Environmental Sciences, E-ISSN 2360-9222, Vol.2, No. 1, June 2025, Published by the Faculty of Environmental Sciences, Plateau State University, Bokkos. https://journals.plasu.edu.ng, DOI: 10.5281/zenodo.21854300

INTEGRATION OF GNSS AND DRONE-DERIVED HIGH RESOLUTION TOPOGRAPHIC SURVEYS IN ENHANCING HIGHWAY GEOMETRIC DESIGN ACCURACY

[1]Geoffrey Ogbonna Nwodo [1]Joseph Olayemi Odumosu

[1] Department of Geomatics, University of Benin, Edo state, Nigeria
Corresponding Author's Email: geoffrey.nwodo@uniben.edu

https://orcid.org/0000-0002-6418-772X

ABSTRACT

This study evaluated the integration of Global Navigation Satellite System (GNSS) and drone-derived high-resolution topographic surveys for highway geometric design along the 4.2 km Upper Mission Extension Road, Benin City, Nigeria. A field-based geospatial engineering approach was adopted, with 17 GNSS Ground Control Points established for horizontal and vertical control. A UAV survey covering 101.72 ha was conducted, during which 3,162 aerial images were acquired and processed to generate orthomosaics, dense point clouds, and Digital Terrain Models (DTMs). The integrated GNSS-UAV dataset was used to develop longitudinal profiles, horizontal alignments, vertical curves, and plan-and-profile drawings for highway geometric design. Performance evaluation involved elevation comparison, Root Mean Square Error (RMSE), mean error, standard deviation, point-density analysis, terrain representation, and highway profile assessment. Results from 169 common survey points showed a mean error of −1.366 m, an RMSE of 1.463 m, and a standard deviation of 0.526 m between the GNSS-only and integrated terrain models. The UAV survey achieved an average Ground Sampling Distance (GSD) of 1.89 cm and generated approximately 232.96 million points, corresponding to a point density of 229.02 points/m², compared with only 169 discrete GNSS observations (0.000166 points/m²) over the same area. The integrated approach produced a more continuous and detailed terrain model, enabling improved identification of terrain undulations, enhanced longitudinal profile development, refined vertical alignment design, and more accurate highway geometric design. The study concludes that integrating GNSS with UAV photogrammetry significantly enhances terrain representation and design accuracy and is recommended for future highway rehabilitation and engineering projects.

Keywords: Integration, Drone-Derived; High Resolution; Topographic Surveys; Enhancing Highway Geometric; Design Accuracy

1. INTRODUCTION

Transportation infrastructure is a fundamental component of economic development, facilitating the movement of people, goods, and services while promoting regional integration and national growth. Among transportation infrastructures, highways remain the dominant mode of land transportation in many developing countries, including Nigeria (Agüera-Vega, Carvajal-Ramírez, & Martínez-Carricondo, 2017). The planning, design, construction, and maintenance of highways require highly accurate geospatial information to ensure safety, structural stability, cost-effectiveness, and long-term operational performance. One of the most critical inputs in highway engineering is the acquisition of reliable topographic data for geometric design (Colomina, & Molina, 2014).

Highway geometric design involves determining the physical dimensions and alignment of road elements, including horizontal curves, vertical curves, gradients, cross-sections, super-elevation, sight distances, and drainage systems. The quality of these design elements depends largely on the precision and completeness of the topographic survey conducted during the planning phase (Luhmann, Robson, Kyle, & Harley, 2020). Errors in terrain representation can result in inaccurate earthwork estimates, poor alignment decisions, increased construction costs, environmental degradation, and compromised road safety.

Traditionally, highway topographic surveys have relied on conventional surveying techniques such as total stations, levels, and Global Navigation Satellite System (GNSS) receivers. GNSS technology has revolutionized geospatial data acquisition by providing accurate three-dimensional positioning through satellite-based navigation systems such as the Global Positioning System (GPS), GLONASS, Galileo, and BeiDou. Modern Real-Time Kinematic (RTK) and Post-Processed Kinematic (PPK) GNSS systems are capable of achieving centimetre-level accuracy under favourable observation conditions (Bang, Habib, Kim, & Kim, 2018). Their efficiency, speed, and precision have made them indispensable tools for engineering surveys, cadastral mapping, deformation monitoring, and highway alignment studies.

Despite these advantages, GNSS surveys possess certain limitations. Signal obstruction by dense vegetation, buildings, bridges, steep terrain, and adverse atmospheric conditions may reduce positional accuracy or completely interrupt satellite reception (James, Robson, d'Oleire-Oltmanns, & Niethammer, 2017). Furthermore, point-based GNSS surveys often require numerous observations to adequately represent complex terrain features, increasing field time and labour requirements. Consequently, there is growing interest in integrating complementary remote sensing technologies capable of rapidly capturing dense spatial information.

Recent advances in Unmanned Aerial Vehicles (UAVs), commonly referred to as drones, have transformed topographic surveying by enabling rapid acquisition of high-resolution aerial imagery (Eltner, et al., 2016). Equipped with high-resolution digital cameras and integrated GNSS and inertial navigation systems, drones can capture overlapping images that are processed using photogrammetric techniques such as Structure-from-Motion (SfM) and Multi-View Stereo (MVS) to generate dense point clouds, Digital Surface Models (DSMs), Digital Terrain Models (DTMs), orthophotos, and three-dimensional terrain representations. Drone technology offers several advantages, including rapid data acquisition, reduced field time, enhanced safety, lower operational costs, and the ability to survey inaccessible or hazardous areas (Wolf, Ghilani, & Wilkinson, 2019).

The integration of GNSS observations with drone-derived topographic datasets has emerged as a promising approach for improving survey accuracy and reliability. GNSS provides highly accurate ground control points (GCPs) and checkpoints that enhance the georeferencing and positional accuracy of drone imagery. Conversely, drone photogrammetry supplies dense spatial coverage that complements the discrete point measurements obtained from GNSS surveys (Luhmann, Robson, Kyle, & Harley, 2020). Together, these technologies provide comprehensive terrain information suitable for accurate highway geometric design.

High-resolution topographic surveys generated through integrated GNSS-drone systems offer significant advantages for highway engineering. They enable more precise determination of road alignment, improved estimation of cut-and-fill volumes, better drainage design, enhanced visualization of terrain constraints, optimized route selection, and reduced construction risks (Nex & Remondino, 2014). Additionally, accurate digital terrain models support Building

Information Modelling (BIM), Geographic Information Systems (GIS), and intelligent transportation systems used in modern infrastructure development.

In Nigeria, rapid urbanization, increasing transportation demands, and expanding road networks necessitate the adoption of advanced geospatial technologies capable of improving engineering design quality. However, conventional topographic surveys remain predominant in many highway projects due to limited awareness, technical capacity, and financial constraints (Colomina & Molina, 2014). Comparative assessments evaluating the combined use of GNSS and drone-derived surveys for highway geometric design under Nigerian conditions remain relatively scarce.

This study therefore seeks to investigate the integration of GNSS and drone-derived high-resolution topographic surveys in enhancing highway geometric design accuracy. The study will evaluate positional accuracy, terrain representation, efficiency, and applicability of integrated survey methods while providing recommendations for their adoption in highway engineering practice.

2. MATERIALS AND METHODS

Description of the Study Corridor

The study corridor is Upper Mission Extension Road in Benin City, Nigeria. The supplied drawings, Figures 1 and 2 show a built-up urban environment with dense residential and commercial development, numerous access roads, roadside structures and changes in alignment. This corridor is defined as a linear roadway segment, including the carriageway and its immediate surrounding terrain, which influences highway design elements such as alignment, slope stability, drainage, and earthworks (Sharma, 2014). The selected corridor starts at approximately 6.362° N, 5.639° E (southern end) and ends at 6.367° N, 5.683° E (northern end). It represents typical Nigerian highway conditions, characterized by flat to gently undulating landscapes with moderate vegetation cover and semi-rural surroundings (Chiabro, Nex, Piatti, & Rinaudo, 2011).

To ensure accurate UAV photogrammetry and georeferencing up to 17 ground control points (GCPs) were strategically established along the 4.2 km corridor at intervals of approximately 0–50 m, with additional points in areas of terrain variation. This GCP density is selected based on UAV flight altitude, camera resolution (20 MP or higher), and corridor terrain complexity to achieve centimeter-level positional accuracy. The integrated drawing covers about 4.2 km of roadway. The terrain rises strongly from the beginning of the alignment, reaches an almost level plateau over a substantial central section and then falls slightly toward the terminal section. The corridor contains several short horizontal deflections and multiple designed vertical curves.

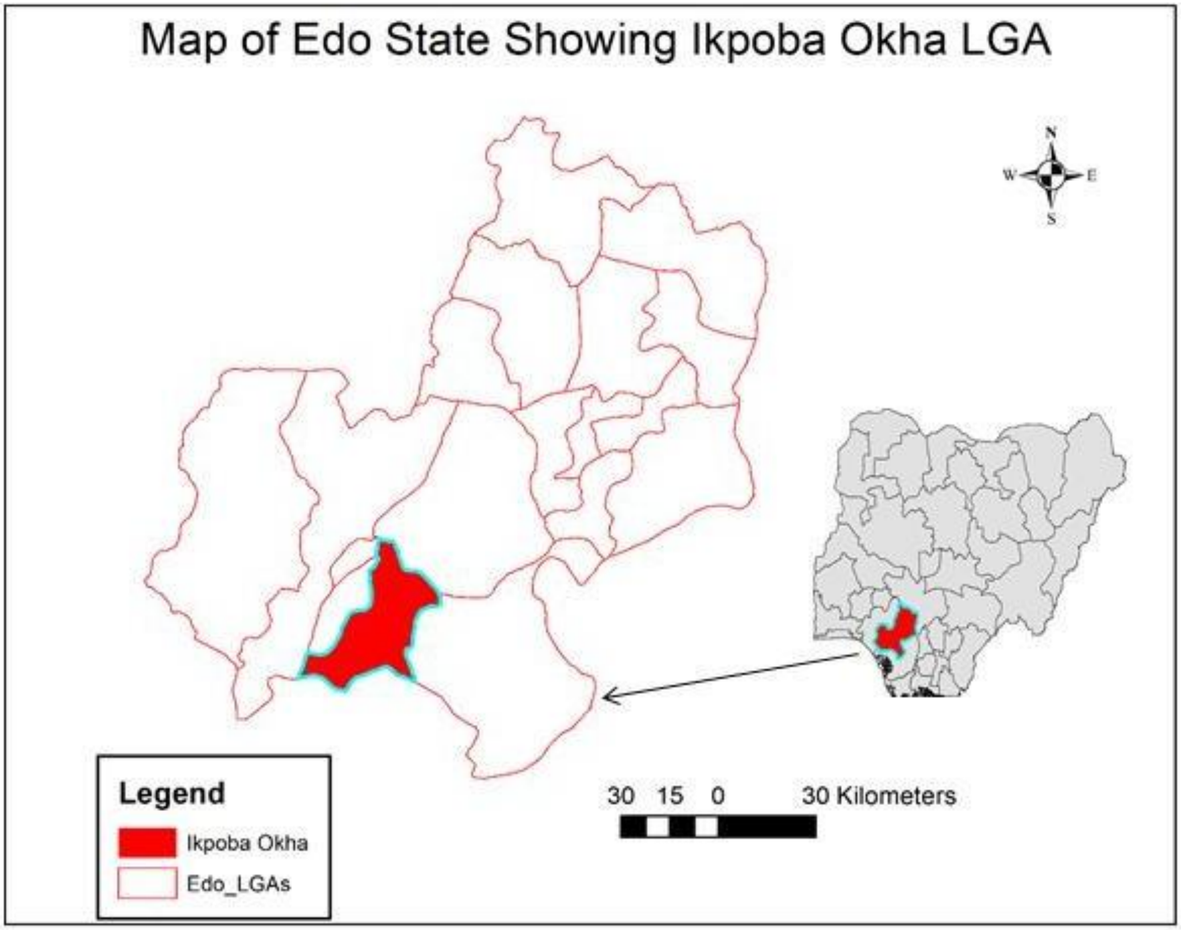

Figure 1: Map of Edo State Showing Ikpoba Okha

Figure 2: Satellite imagery showing the Study Corridor from Upper Mission (GoogleEarth Pro)

Research Design

A sequential integration design was employed. First, GNSS control was established and used to define the project coordinate and elevation reference. Second, drone imagery was acquired over the corridor using flight parameters selected to provide adequate overlap and ground sampling density. Third, the imagery was processed by structure-from-motion and multi-view-stereo photogrammetric procedures. Fourth, the GNSS control was introduced into the photogrammetric adjustment to georeference and constrain the image block. Fifth, the GNSS-derived points and drone-derived surface products were imported into a common civil-design environment. Finally, the combined data were used to produce the plan-and-profile sheets and the geometric design parameters presented in the supplied drawing.

Reconnaissance and Survey Planning

Reconnaissance was undertaken before data acquisition to identify the corridor limits, suitable locations for control points, flight hazards, obstructions, traffic conditions, built-up areas and possible take-off and landing locations. Particular attention was given to the visibility, stability and security of GNSS control marks. The reconnaissance also identified sections with trees, high buildings or narrow spaces that could create GNSS multipath or image occlusion. The survey plan divided the corridor into manageable flight blocks and ground-control zones. The intended final products determined the required spatial resolution, image overlap, flight height and density of ground control. Weather, cloud cover, wind and sun angle were considered because they influence image sharpness, shadows and flight safety.

GNSS DATA ACQUISITION PROCEDURES

Establishment of Project Control

A project control network was established along or close to the road corridor. One or more stable stations were selected as reference stations, while additional control points were distributed to provide geometric strength throughout the corridor. The control points were positioned so that they could serve both conventional GNSS observations and drone ground control. Where a base-rover configuration was used, the base receiver occupied a known or independently determined control point and the rover observed the remaining control and detail points.

Each point was assigned a unique identifier and documented with a description, monument type, occupation time, antenna height and field sketch or photograph. Observations were made with clear satellite visibility where practicable. Points affected by poor satellite geometry, multipath or cycle slips were re-observed.

Coordinate and Elevation Reference

All GNSS observations were reduced to a single project coordinate reference system and vertical datum. Antenna heights were applied correctly during processing. Where ellipsoidal heights were observed, an appropriate geoid model or project benchmark relationship was required to obtain orthometric heights suitable for highway design. Consistent units and datum definitions were maintained during export to photogrammetric and civil-design software.

GNSS topographic observations

The GNSS rover was used to observe accessible road features and independent check points. Typical observations included centreline points, pavement edges, shoulders, junctions, drainage structures, culvert locations, break lines, road furniture and selected terrain points. The GNSS survey also supplied check elevations that could be compared with the drone-derived terrain surface. The observations were coded in the field to support automated line work and feature classification during processing.

GNSS quality control

Quality control involved checking solution status, satellite geometry, number of satellites, occupation duration, coordinate repeatability and closure to known or re-observed points. Fixed integer solutions were preferred for real-time kinematic observations. Repeated occupations were compared to detect blunders. For a complete final thesis, the GNSS results table should contain point identification, easting, northing, elevation, horizontal precision, vertical precision and repeat-observation differences.

DRONE DATA ACQUISITION PROCEDURES

Ground-control and check-point arrangement

Clearly visible aerial targets were placed and surveyed with GNSS before the flight. Ground-control points were distributed near the beginning and end of each block, along both sides of the corridor and within the interior of longer blocks. Independent check points were withheld from the photogrammetric adjustment and used only for accuracy assessment. This separation is necessary because control-point residuals alone do not provide an independent measure of mapping accuracy.

Flight planning

The flight plan was designed to achieve continuous stereoscopic coverage of the road and adjacent features. High forward and side overlap were selected to support reliable image matching in an urban corridor. The flight altitude was selected with reference to the desired ground sampling distance, legal restrictions, obstacle clearance and camera characteristics. The camera was oriented predominantly at nadir, while additional oblique imagery could be acquired where buildings or trees created occlusions.

Flights were preferably conducted in stable weather with low wind, adequate illumination and minimal precipitation. Pre-flight checks covered batteries, propellers, storage media, firmware, navigation status, return-to-home altitude and airspace restrictions. A visual observer and safe operating area were used where required.

Image acquisition and field checks

During the flight, image triggering, flight path, overlap and battery status were monitored. After each block, the imagery was checked for blur, exposure problems, missing strips and inadequate overlap. Defective blocks were reflown before leaving the site. The image files and field records were backed up and organized by flight block.

Photogrammetric Processing

The drone images were processed through the standard photogrammetric sequence: image import and quality screening; camera alignment and tie-point extraction; initial bundle adjustment; introduction of GNSS-surveyed ground control; optimization of camera parameters and image exterior orientation; dense point-cloud generation; point classification and editing; DSM and, where required, bare-earth DTM generation; orthorectification and orthomosaic production; contour and break-line extraction; and export to the project coordinate system.

Road surfaces require careful classification because vehicles, vegetation, temporary objects and building edges can contaminate an unedited surface. Manual editing and break lines were therefore required around the road edges, drains and abrupt elevation changes. The orthomosaic provided planimetric context, while the edited terrain model supplied elevations for profile and cross-section extraction.

Integration of GNSS and Drone Data

Integration was performed in a common coordinate system. The GNSS control constrained the drone model, and the independent GNSS check points were compared with corresponding elevations or identifiable points in the drone products. GNSS-observed break points were retained where direct field measurement was considered more reliable than image matching. The drone point cloud supplied dense coverage between these points. Duplicate or conflicting observations were inspected rather than averaged automatically.

The combined dataset was imported into civil-design software to form the existing ground surface. An alignment was then fitted to the mapped road corridor. Chainages, tangent sections, horizontal curves, longitudinal grades, vertical points of intersection and vertical curves were generated. Existing ground elevations and finished design elevations were sampled at 25 m intervals for the plan-and-profile sheets.

Highway Geometric Design Procedure

The geometric design procedure comprised: definition of the road centreline; assignment of chainage; identification of tangent intersections; insertion of horizontal curves at directional changes; extraction of the existing longitudinal profile from the integrated terrain model; selection of design grades; location of vertical points of intersection; design of crest and sag curves; and generation of finished profile levels. The supplied sheets show horizontal curve start and end stations using PC and PT notation and provide separate vertical-curve details using PVI, BVC/BVCS, EVC/EVCS, algebraic grade difference and K values.

The project profile was designed to follow the terrain while improving continuity and constructability. The early section contains strong positive grades, the central section is nearly level and the terminal section includes a slight negative grade. Vertical curves were introduced at grade changes to smooth the profile.

Accuracy Assessment and Statistical Analysis

Accuracy assessment should be conducted separately for the GNSS survey, drone survey and integrated surface. The following statistics are recommended:

Mean error: $ME = (1/n)\ \Sigma(e_i)$

Root mean square error: $RMSE = \sqrt{[(1/n)\ \Sigma(e_i^2)]}$

Horizontal positional error: $RMSE_r = \sqrt{(RMSE_x^2 + RMSE_Y^2)}$

Standard deviation: $s = \sqrt{[\Sigma(e_i - \bar{e})^2/(n-1)]}$

For GNSS, repeated occupations and closures provide internal checks. For the drone model, errors at independent check points provide external accuracy. For the integrated model, residuals between GNSS check elevations and the final terrain surface, profile smoothness and consistency at overlap zones provide the principal checks. Outliers should be investigated and reported rather than removed without justification.

Data Presentation

Results were organized into three distinct categories as required by the research objectives: (1) GNSS-only results, representing the control network and directly observed points; (2) drone-only results, representing imagery-derived products before final integration; and (3) integrated GNSS-drone results, represented by the final plan-and-profile drawings and vertical-curve schedule. This separation permits the contribution of each technology to be evaluated before assessing the combined method.

3. RESULTS AND DISCUSSION

Elevation Difference Data

Table 1 compares elevations obtained from the GNSS-only survey and the integrated GNSS + drone high-resolution topographic survey along a 4.2 km highway alignment. At the starting chainage (0+000), both methods produced the same elevation of 66.068 m, resulting in zero elevation difference, which indicates perfect agreement at the control point. Small positive differences were observed between chainages 0+025 and 0+050, where the integrated survey recorded elevations 0.258 m and 0.265 m higher than the GNSS survey. Thereafter, the elevation differences became predominantly negative, indicating that the integrated GNSS + drone survey generally produced lower elevation values than the standalone GNSS survey.

The magnitude of the elevation differences increased progressively along the alignment. Moderate differences ranging from approximately −0.5 m to −1.5 m were observed between chainages 0+100 and 1+600, while the largest discrepancies occurred between 0+650 and 0+825, where the maximum negative elevation difference of −2.725 m was recorded at chainage 0+750. Beyond this section, the elevation differences remained relatively consistent, generally ranging between −1.0 m and −2.0 m until the end of the survey at chainage 4+200, where a difference of −1.850 m was observed. The results indicate that the integrated GNSS + drone survey generated a smoother and more consistent terrain model than the GNSS-only survey by capturing subtle variations in ground elevation that may not have been adequately represented by point-based GNSS observations alone. The observed elevation differences demonstrate the added value of integrating drone-derived high-resolution topographic data with GNSS measurements for improving terrain representation and enhancing the accuracy of highway geometric design, particularly in areas with complex surface characteristics.

Table 1: **Elevation Difference Data**

S/N	**CHAINAGE**	**GNSS Elevation Survey Data**	**GNSS + Drone Survey Elevation Data**	**Elevation Difference**
1	0+000	66.068	66.068	0.000
2	0+025	66.843	67.101	0.258
3	0+050	67.943	68.208	0.265
4	0+075	69.993	69.341	-0.652
5	0+100	71.818	70.541	-1.277
6	0+125	72.868	71.917	-0.951
7	0+150	74.293	73.436	-0.857
8	0+175	75.843	74.982	-0.861
9	0+200	77.343	76.547	-0.796
10	0+225	78.818	78.053	-0.765
11	0+250	80.243	79.581	-0.662
12	0+275	81.443	81.040	-0.403
13	0+300	82.568	82.436	-0.132
14	0+325	84.143	83.769	-0.374
15	0+350	84.993	84.951	-0.042
16	0+375	86.618	86.121	-0.497
17	0+400	87.743	87.269	-0.474
18	0+425	88.868	88.382	-0.486
19	0+450	89.818	89.534	-0.284
20	0+475	91.018	90.771	-0.247
21	0+500	92.568	91.981	-0.587
22	0+525	93.943	93.212	-0.731
23	0+550	95.868	94.434	-1.434
24	0+575	97.293	95.786	-1.507
25	0+600	98.793	97.166	-1.627
26	0+625	99.618	98.498	-1.120
27	0+650	101.843	99.885	-1.958
28	0+675	103.418	101.284	-2.134
29	0+700	104.968	102.771	-2.197
30	0+725	106.168	104.205	-1.963
31	0+750	108.318	105.593	-2.725
32	0+775	109.168	107.027	-2.141
33	0+800	110.593	108.524	-2.069
34	0+825	112.118	109.972	-2.146
35	0+850	113.193	111.388	-1.805
36	0+875	114.218	112.709	-1.509
37	0+900	115.393	113.934	-1.459
38	0+925	116.343	115.122	-1.221
39	0+950	117.468	116.273	-1.195
40	0+975	118.643	117.352	-1.291

41	1+000	119.568	118.338	-1.230
42	1+025	120.418	119.273	-1.145
43	1+050	121.093	120.194	-0.899
44	1+075	121.468	120.978	-0.490
45	1+100	122.318	121.660	-0.658
46	1+125	122.968	122.292	-0.676
47	1+150	123.343	122.811	-0.532
48	1+175	123.218	123.188	-0.030
49	1+200	124.543	123.456	-1.087
50	1+225	124.568	123.597	-0.971
51	1+250	124.443	123.615	-0.828
52	1+275	124.718	123.602	-1.116
53	1+300	124.293	123.605	-0.688
54	1+325	124.168	123.600	-0.568
55	1+350	124.493	123.629	-0.864
56	1+375	124.768	123.629	-1.139
57	1+400	124.518	123.616	-0.902
58	1+425	124.893	123.585	-1.308
59	1+450	125.093	123.611	-1.482
60	1+475	125.293	123.617	-1.676
61	1+500	125.243	123.610	-1.633
62	1+525	125.143	123.638	-1.505
63	1+550	125.068	123.638	-1.430
64	1+575	125.143	123.667	-1.476
65	1+600	125.218	123.662	-1.556
66	1+625	125.243	123.712	-1.531
67	1+650	125.393	123.695	-1.698
68	1+675	125.293	123.714	-1.579
69	1+700	125.193	123.707	-1.486
70	1+725	125.368	123.702	-1.666
71	1+750	125.393	123.735	-1.658
72	1+775	125.118	123.726	-1.392
73	1+800	125.368	123.760	-1.608
74	1+825	125.343	123.765	-1.578
75	1+850	125.518	123.761	-1.757
76	1+875	125.693	123.743	-1.950
77	1+900	125.468	123.791	-1.677
78	1+925	125.518	123.771	-1.747
79	1+950	125.543	123.782	-1.761
80	1+975	125.568	123.783	-1.785
81	2+000	125.543	123.804	-1.739
82	2+025	125.468	123.820	-1.648
83	2+050	125.493	123.830	-1.663

PLATEAU STATE UNIVERSITY, BOKKOS
Established 2005
Knowledge, Diligence, Service

84	2+075	125.468	123.825	-1.643
85	2+100	125.493	123.840	-1.653
86	2+125	125.518	123.867	-1.651
87	2+150	125.443	123.878	-1.565
88	2+175	125.543	123.898	-1.645
89	2+200	125.818	123.884	-1.934
90	2+225	125.693	123.940	-1.753
91	2+250	125.568	123.945	-1.623
92	2+275	125.768	123.958	-1.810
93	2+300	125.568	123.972	-1.596
94	2+325	125.518	123.958	-1.560
95	2+350	125.718	124.010	-1.708
96	2+375	125.893	124.050	-1.843
97	2+400	125.843	124.015	-1.828
98	2+425	125.893	124.064	-1.829
99	2+450	125.768	124.039	-1.729
100	2+475	126.193	124.065	-2.128
101	2+500	125.818	124.061	-1.757
102	2+525	125.943	124.061	-1.882
103	2+550	126.143	124.068	-2.075
104	2+575	125.593	124.089	-1.504
105	2+600	125.568	124.124	-1.444
106	2+625	125.493	124.100	-1.393
107	2+650	125.468	124.085	-1.383
108	2+675	125.343	124.041	-1.302
109	2+700	125.368	124.107	-1.261
110	2+725	125.343	124.100	-1.243
111	2+750	125.368	124.102	-1.266
112	2+775	125.568	124.121	-1.447
113	2+800	125.418	124.131	-1.287
114	2+825	125.593	124.150	-1.443
115	2+850	125.218	124.175	-1.043
116	2+875	125.543	124.161	-1.382
117	2+900	124.968	124.170	-0.798
118	2+925	125.343	124.183	-1.160
119	2+950	125.893	124.202	-1.691
120	2+975	126.018	124.184	-1.834
121	3+000	126.043	124.200	-1.843
122	3+025	125.718	124.218	-1.500
123	3+050	125.643	124.214	-1.429
124	3+075	125.618	124.225	-1.393
125	3+100	125.643	124.270	-1.373
126	3+125	125.568	124.279	-1.289
127	3+150	125.468	124.314	-1.154

PLATEAU STATE UNIVERSITY, BOKKOS
Established 2005
Knowledge, Diligence, Service

128	3+175	125.543	124.290	-1.253
129	3+200	125.518	124.281	-1.237
130	3+225	125.568	124.273	-1.295
131	3+250	125.393	124.304	-1.089
132	3+275	125.343	124.308	-1.035
133	3+300	125.368	124.331	-1.037
134	3+325	125.418	124.343	-1.075
135	3+350	125.518	124.328	-1.190
136	3+375	125.793	124.349	-1.444
137	3+400	126.043	124.310	-1.733
138	3+425	126.368	124.379	-1.989
139	3+450	126.568	124.414	-2.154
140	3+475	126.543	124.461	-2.082
141	3+500	126.268	124.440	-1.828
142	3+525	126.293	124.426	-1.867
143	3+550	126.368	124.460	-1.908
144	3+575	126.493	124.430	-2.063
145	3+600	126.268	124.459	-1.809
146	3+625	126.418	124.476	-1.942
147	3+650	126.393	124.475	-1.918
148	3+675	126.343	124.455	-1.888
149	3+700	126.218	124.474	-1.744
150	3+725	126.143	124.470	-1.673
151	3+750	126.118	124.465	-1.653
152	3+775	125.993	124.469	-1.524
153	3+800	125.968	124.528	-1.440
154	3+825	126.043	124.478	-1.565
155	3+850	126.018	124.518	-1.500
156	3+875	125.968	124.537	-1.431
157	3+900	126.068	124.545	-1.523
158	3+925	126.118	124.585	-1.533
159	3+950	126.068	124.576	-1.492
160	3+975	126.143	124.575	-1.568
161	4+000	126.243	124.572	-1.671
162	4+025	125.993	124.552	-1.441
163	4+050	126.093	124.570	-1.523
164	4+075	125.718	124.538	-1.180
165	4+100	125.218	124.450	-0.768
166	4+125	125.268	124.286	-0.982
167	4+150	125.143	124.226	-0.917
168	4+175	126.118	124.090	-2.028
169	4+200	125.868	124.018	-1.850

PLATEAU STATE UNIVERSITY, BOKKOS
Established 2005
Knowledge, Diligence, Service

RMSE Data

Table 2 presents the point-by-point elevation errors between the GNSS-only survey and the integrated GNSS + drone survey, which were used to evaluate the vertical accuracy of the topographic data. At the control point (Station 1), both methods recorded the same elevation (66.068 m), resulting in zero error, while only two stations (Stations 2 and 3) showed small positive errors of 0.258 m and 0.265 m, indicating slightly higher elevations from the integrated survey. From Station 4 onward, the calculated errors were predominantly negative, indicating that the integrated GNSS + drone survey consistently produced slightly lower elevation values than the GNSS-only survey.

The magnitude of the errors increased gradually along the survey corridor. The largest negative error (−2.725 m) occurred at Station 31, after which the errors remained relatively stable, generally ranging between −1.2 m and −2.0 m for most of the remaining stations. Towards the end of the alignment, the calculated errors fluctuated within this range, with the final station (Station 169) recording an error of −1.850 m. The relatively consistent error pattern suggests that the differences between the two datasets were systematic rather than random. The RMSE analysis indicates good consistency between the GNSS-only and integrated GNSS + drone datasets while demonstrating that the integration of drone-derived topographic information provides a refined representation of terrain elevation. The observed systematic differences reflect the ability of drone photogrammetry to capture detailed surface characteristics that may not be fully represented by discrete GNSS observations alone, thereby enhancing the accuracy and reliability of topographic data for highway geometric design, earthwork estimation, and engineering decision-making.

Table 2: RMSE Data

S/N	GNSS Elevation Survey Data	GNSS + Drone Survey Elevation Data	Calculated Error
1	66.068	66.068	0.000
2	66.843	67.101	0.258
3	67.943	68.208	0.265
4	69.993	69.341	-0.652
5	71.818	70.541	-1.277
6	72.868	71.917	-0.951
7	74.293	73.436	-0.857
8	75.843	74.982	-0.861
9	77.343	76.547	-0.796
10	78.818	78.053	-0.765
11	80.243	79.581	-0.662
12	81.443	81.040	-0.403
13	82.568	82.436	-0.132
14	84.143	83.769	-0.374
15	84.993	84.951	-0.042
16	86.618	86.121	-0.497
17	87.743	87.269	-0.474
18	88.868	88.382	-0.486

19	89.818	89.534	-0.284
20	91.018	90.771	-0.247
21	92.568	91.981	-0.587
22	93.943	93.212	-0.731
23	95.868	94.434	-1.434
24	97.293	95.786	-1.507
25	98.793	97.166	-1.627
26	99.618	98.498	-1.120
27	101.843	99.885	-1.958
28	103.418	101.284	-2.134
29	104.968	102.771	-2.197
30	106.168	104.205	-1.963
31	108.318	105.593	-2.725
32	109.168	107.027	-2.141
33	110.593	108.524	-2.069
34	112.118	109.972	-2.146
35	113.193	111.388	-1.805
36	114.218	112.709	-1.509
Cont'd			
37	115.393	113.934	-1.459
38	116.343	115.122	-1.221
39	117.468	116.273	-1.195
40	118.643	117.352	-1.291
41	119.568	118.338	-1.230
42	120.418	119.273	-1.145
43	121.093	120.194	-0.899
44	121.468	120.978	-0.490
45	122.318	121.660	-0.658
46	122.968	122.292	-0.676
47	123.343	122.811	-0.532
48	123.218	123.188	-0.030
49	124.543	123.456	-1.087
50	124.568	123.597	-0.971
51	124.443	123.615	-0.828
52	124.718	123.602	-1.116
53	124.293	123.605	-0.688
54	124.168	123.600	-0.568
55	124.493	123.629	-0.864
56	124.768	123.629	-1.139
57	124.518	123.616	-0.902
58	124.893	123.585	-1.308
59	125.093	123.611	-1.482
60	125.293	123.617	-1.676
61	125.243	123.610	-1.633

62	125.143	123.638	-1.505
63	125.068	123.638	-1.430
64	125.143	123.667	-1.476
65	125.218	123.662	-1.556
66	125.243	123.712	-1.531
67	125.393	123.695	-1.698
68	125.293	123.714	-1.579
69	125.193	123.707	-1.486
70	125.368	123.702	-1.666
71	125.393	123.735	-1.658
72	125.118	123.726	-1.392
73	125.368	123.760	-1.608
74	125.343	123.765	-1.578
75	125.518	123.761	-1.757
76	125.693	123.743	-1.950
77	125.468	123.791	-1.677
78	125.518	123.771	-1.747
79	125.543	123.782	-1.761
80	125.568	123.783	-1.785
81	125.543	123.804	-1.739
82	125.468	123.820	-1.648
Cont'd			
83	125.493	123.830	-1.663
84	125.468	123.825	-1.643
85	125.493	123.840	-1.653
86	125.518	123.867	-1.651
87	125.443	123.878	-1.565
88	125.543	123.898	-1.645
89	125.818	123.884	-1.934
90	125.693	123.940	-1.753
91	125.568	123.945	-1.623
92	125.768	123.958	-1.810
93	125.568	123.972	-1.596
94	125.518	123.958	-1.560
95	125.718	124.010	-1.708
96	125.893	124.050	-1.843
97	125.843	124.015	-1.828
98	125.893	124.064	-1.829
99	125.768	124.039	-1.729
100	126.193	124.065	-2.128
101	125.818	124.061	-1.757
102	125.943	124.061	-1.882
103	126.143	124.068	-2.075
104	125.593	124.089	-1.504

105	125.568	124.124	-1.444
106	125.493	124.100	-1.393
107	125.468	124.085	-1.383
108	125.343	124.041	-1.302
109	125.368	124.107	-1.261
110	125.343	124.100	-1.243
111	125.368	124.102	-1.266
112	125.568	124.121	-1.447
113	125.418	124.131	-1.287
114	125.593	124.150	-1.443
115	125.218	124.175	-1.043
116	125.543	124.161	-1.382
117	124.968	124.170	-0.798
118	125.343	124.183	-1.160
119	125.893	124.202	-1.691
120	126.018	124.184	-1.834
121	126.043	124.200	-1.843
122	125.718	124.218	-1.500
123	125.643	124.214	-1.429
124	125.618	124.225	-1.393
125	125.643	124.270	-1.373
126	125.568	124.279	-1.289
127	125.468	124.314	-1.154
128	125.543	124.290	-1.253
129	125.518	124.281	-1.237
130	125.568	124.273	-1.295
131	125.393	124.304	-1.089
132	125.343	124.308	-1.035
133	125.368	124.331	-1.037
134	125.418	124.343	-1.075
135	125.518	124.328	-1.190
136	125.793	124.349	-1.444
137	126.043	124.310	-1.733
138	126.368	124.379	-1.989
139	126.568	124.414	-2.154
140	126.543	124.461	-2.082
141	126.268	124.440	-1.828
142	126.293	124.426	-1.867
143	126.368	124.460	-1.908
144	126.493	124.430	-2.063
145	126.268	124.459	-1.809
146	126.418	124.476	-1.942
147	126.393	124.475	-1.918
148	126.343	124.455	-1.888

149	126.218	124.474	-1.744
150	126.143	124.470	-1.673
151	126.118	124.465	-1.653
152	125.993	124.469	-1.524
153	125.968	124.528	-1.440
154	126.043	124.478	-1.565
155	126.018	124.518	-1.500
156	125.968	124.537	-1.431
157	126.068	124.545	-1.523
158	126.118	124.585	-1.533
159	126.068	124.576	-1.492
160	126.143	124.575	-1.568
161	126.243	124.572	-1.671
162	125.993	124.552	-1.441
163	126.093	124.570	-1.523
164	125.718	124.538	-1.180
165	125.218	124.450	-0.768
166	125.268	124.286	-0.982
167	125.143	124.226	-0.917
168	126.118	124.090	-2.028
169	125.868	124.018	-1.850

Summary of RMSE Analysis

Table 3 summarizes the statistical evaluation of the elevation differences between the GNSS-only survey and the integrated GNSS + drone survey based on 169 observation points. The analysis produced a mean error of −1.366 m, indicating that, on average, the integrated GNSS + drone survey generated slightly lower elevation values than the GNSS-only survey. The Root Mean Square Error (RMSE) of 1.463 m reflects the overall vertical discrepancy between the two datasets and indicates a good level of agreement for engineering applications, while the standard deviation of 0.526 m suggests that the elevation differences were relatively consistent with limited variability across the survey corridor. The results also show that the maximum positive elevation difference was +0.265 m, whereas the maximum negative difference reached −2.725 m, demonstrating that the largest discrepancies were associated with lower elevations obtained from the integrated survey. The predominance of negative errors indicates a systematic trend rather than random measurement noise, suggesting that the drone-derived high-resolution terrain model captured subtle variations in the ground surface that were not fully represented by the discrete GNSS observations. The RMSE statistics demonstrate that integrating GNSS measurements with drone-derived topographic data enhances the consistency and reliability of terrain modelling. The relatively low RMSE and standard deviation indicate that the integrated approach is suitable for high-precision highway geometric design, providing improved terrain representation, more reliable earthwork computations, and better support for engineering decision-making compared with the use of GNSS observations alone.

Table 3: Summary of RMSE Analysis

Parameter	Value
Number of Points (n)	169
Mean Error	-1.366 m
RMSE	1.463 m
Standard Deviation	0.526 m
Maximum Positive Difference	+0.265 m
Maximum Negative Difference	-2.725 m

Comparison of Survey Point Density

Table 4 compares the spatial data resolution obtained from the GNSS survey and the integrated GNSS–UAV (drone) survey over the same survey area of 1,017,200 m². The conventional GNSS survey recorded only 169 survey points, corresponding to a point density of 0.000166 points/m² (or 1.66 points/ha), reflecting the discrete nature of point-based ground surveying. In contrast, the integrated GNSS–UAV survey generated 232,962,347 survey points, yielding a remarkably higher point density of 229.02 points/m² (or 2,290,217 points/ha), representing an increase of more than 1.3 million times compared with the conventional GNSS survey. The substantially higher point density achieved by the integrated GNSS–UAV survey demonstrates its ability to capture detailed terrain features continuously across the entire highway corridor rather than at isolated observation points. This dense spatial coverage enables the production of high-resolution digital terrain models, more accurate contour maps, improved representation of subtle topographic variations, and enhanced identification of terrain irregularities that may influence highway alignment and drainage design. The results indicate that integrating GNSS with UAV photogrammetry significantly improves topographic data resolution and surface representation. The dramatic increase in survey point density enhances the precision of highway geometric design, earthwork volume estimation, slope analysis, and engineering decision-making, making the integrated approach more suitable for modern highway surveying and infrastructure development than conventional GNSS surveying alone.

Table 4: Comparison of Survey Point Density

Parameter	GNSS Survey	GNSS-UAV Survey
Number of Points	169	232,962,347
Survey Area (m²)	1,017,200	1,017,200
Point Density (points/m²)	0.000166	229.02
Point Density (points/ha)	1.66	2,290,217

UAV Survey Outputs

Table 5 presents the operational outputs of the UAV survey conducted over a 101.72 ha highway corridor. A total of 3,162 aerial images were captured during the survey, of which 3,150 images were successfully calibrated for photogrammetric processing, representing a calibration success rate of approximately 99.6%. This high calibration rate indicates excellent image quality, adequate overlap, and successful camera orientation, providing a reliable dataset for generating accurate topographic products. The survey achieved an average Ground Sampling Distance (GSD) of 1.89 cm, indicating that each image pixel represents approximately 1.89 cm on the ground. Such a high spatial resolution enables the detection of fine terrain details and small surface features, allowing for the production of highly accurate digital terrain models, orthophotos, and three-dimensional surface representations required for highway engineering. The UAV survey outputs demonstrate the effectiveness of drone photogrammetry in acquiring dense, high-resolution geospatial data over large areas within a relatively short time. The combination of extensive image coverage, high calibration success, and a very fine GSD confirms that the UAV-derived dataset is well suited for enhancing highway geometric design accuracy, improving terrain modelling, and supporting precise engineering analyses.

Table 5: UAV Survey Outputs

Parameter	**Value**
Survey Area	101.72*ha*
Total Images Captured	3,162
Calibrated Images	3,150
Average Ground Sampling Distance (GSD)	1.89 cm

Digital Terrain Model (DTM)

Figure 1 presents the Digital Terrain Model (DTM) generated from the three UAV survey blocks covering the study corridor. The integrated terrain model provides a continuous three-dimensional representation of the ground surface, with the colour gradient illustrating variations in elevation along the highway alignment. Lower elevations are represented by the cooler colours (green and light blue), while higher elevations are depicted by warmer colours (yellow and orange), indicating gradual changes in terrain relief across the surveyed area. The DTM demonstrates the successful integration of the three UAV survey blocks into a seamless terrain surface with no obvious discontinuities between adjacent blocks. The model captures subtle topographic variations, changes in slope, embankments, and natural ground undulations that would be difficult to represent using conventional point-based GNSS surveys alone. The continuity and high spatial resolution of the terrain model indicate effective photogrammetric processing and accurate georeferencing of the UAV imagery. Figure 1 highlights the capability of UAV photogrammetry to generate detailed and high-resolution digital terrain models suitable for highway engineering applications. The terrain model provides a reliable basis for highway geometric design, route alignment optimization, earthwork volume computation, drainage planning, slope stability assessment, and other engineering analyses. The integration of GNSS control with UAV-derived topographic data therefore enhances terrain representation and improves the accuracy and efficiency of highway design and construction planning.

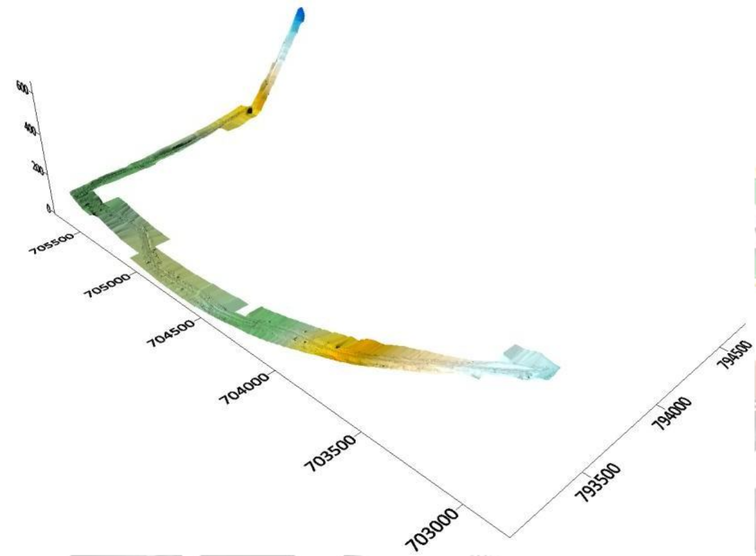

Figures 1: Digital Terrain Models generated from the three UAV survey blocks.

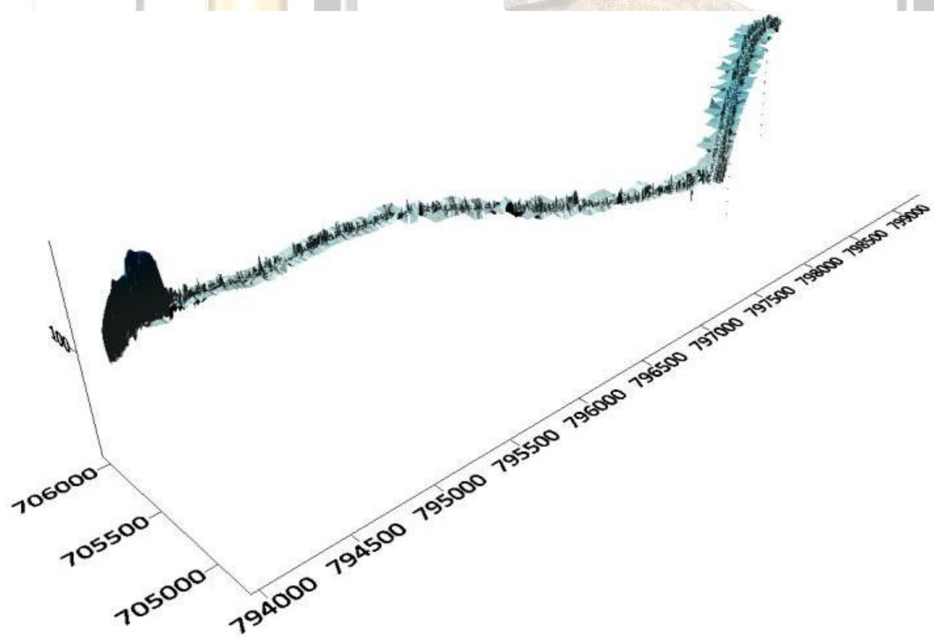

Figure 2: Digital Terrain Model (DTM) of Temboga 1.

SITY, BOKKOS
Establlished 2005

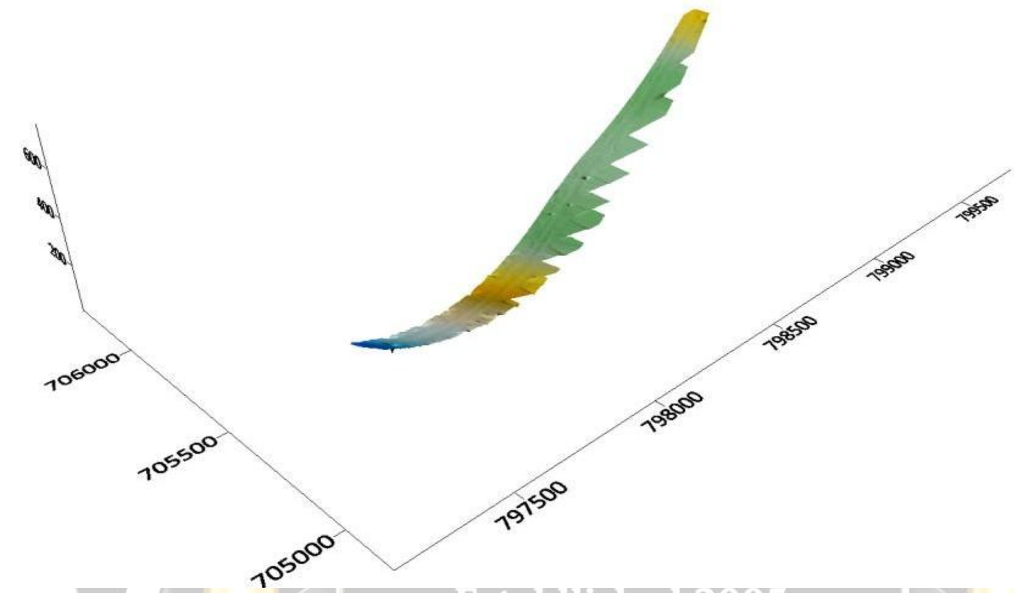

Figure 3: Digital Terrain Model (DTM) of Temboga 3.

Point Density Comparison

Table 6 compares the spatial sampling density achieved by the conventional GNSS survey and the integrated GNSS–UAV survey. The conventional GNSS survey collected 169 observation points, corresponding to a point density of 0.000166 points/m², reflecting the discrete and widely spaced nature of ground-based measurements. In contrast, the integrated GNSS–UAV survey generated an exceptionally dense dataset comprising 232,962,347 points, resulting in a point density of 229.02 points/m². The results reveal a dramatic improvement in spatial resolution when UAV photogrammetry is integrated with GNSS control. While the GNSS survey provides accurate point coordinates at selected locations, the integrated GNSS–UAV approach captures a nearly continuous representation of the terrain surface by recording millions of closely spaced elevation points. This dense point cloud enables the accurate modelling of subtle terrain variations, road embankments, drainage channels, and other surface features that may be missed by conventional point-based surveys. Overall, the comparison demonstrates that integrating UAV photogrammetry with GNSS significantly enhances the density and quality of topographic data. The substantial increase in point density improves the accuracy of digital terrain modelling, highway alignment design, earthwork volume estimation, and other engineering analyses, making the integrated GNSS–UAV approach more suitable for modern highway surveying and geometric design than the use of GNSS surveying alone.

Table 6: Point Density Comparison

Parameter	GNSS Survey	Integrated GNSS-UAV Survey
Number of Points	169	232,962,347
Point Density (points/m²)	0.000166	229.02

Comparison of Terrain Representation

Table 7 compares the quality of terrain representation obtained from the conventional GNSS survey and the integrated GNSS + UAV survey. Both methods utilized 169 GNSS control points; however, while the conventional GNSS survey relied solely on these discrete observations, the integrated GNSS + UAV survey complemented the control points with a dense point cloud of 232,962,347 points. This substantial increase in data density enabled the generation of a much more comprehensive representation of the terrain surface. The conventional GNSS survey provided moderate spatial resolution and moderate terrain detail, with the ground surface being represented through interpolation between individual survey points. In contrast, the integrated GNSS + UAV survey achieved very high spatial resolution and excellent terrain detail, as the terrain surface was directly measured through high-density photogrammetric observations. This approach captured subtle variations in elevation, slopes, embankments, drainage channels, and other surface features that are often overlooked or generalized in conventional GNSS surveys. The results demonstrate that integrating GNSS with UAV photogrammetry significantly improves terrain representation by producing a dense, high-resolution, and directly measured surface model. This enhanced terrain information provides a more accurate basis for highway geometric design, route optimization, earthwork volume estimation, drainage analysis, and other engineering applications, highlighting the superiority of the integrated approach over conventional GNSS surveying alone.

Table 7: Comparison of Terrain Representation

Parameter	GNSS Survey	GNSS + UAV Survey
Number of Survey Points	169	169 Control Points
Dense Point Cloud	Not Available	232,962,347 Points
Spatial Resolution	Moderate	Very High
Terrain Detail	Moderate	Excellent
Surface Representation	Interpolated	Directly Measured

Elevation Statistics

Table 8 compares the terrain representation capabilities of the conventional GNSS survey and the integrated GNSS + UAV survey. Although both methods were referenced using 169 GNSS control points, the integrated GNSS + UAV survey generated a dense point cloud comprising 232,962,347 points, whereas the conventional GNSS survey did not produce a dense point cloud. This demonstrates the significant enhancement in data acquisition achieved through UAV photogrammetry. The GNSS survey provided moderate spatial resolution and moderate terrain detail, relying on interpolation between discrete survey points to model the ground surface. In contrast, the integrated GNSS + UAV survey achieved very high spatial resolution and excellent terrain detail by directly measuring the terrain using millions of photogrammetrically derived points. This high-density dataset enabled the accurate representation of subtle changes in topography, including slopes, depressions, embankments, and drainage features. The comparison confirms that the integration of GNSS with UAV photogrammetry substantially improves the quality of terrain representation. The enhanced spatial resolution and detailed surface information produced by the integrated approach provide a more accurate and reliable foundation for highway geometric design, earthwork calculations, drainage planning, and other engineering applications compared with the conventional GNSS survey.

Table 8: Elevation Statistics

Parameter	GNSS Survey	GNSS + UAV Survey
Number of Survey Points	169	169 Control Points
Dense Point Cloud	Not Available	232,962,347 Points
Spatial Resolution	Moderate	Very High
Terrain Detail	Moderate	Excellent

The findings of this study demonstrate that the integration of Global Navigation Satellite System (GNSS) and Unmanned Aerial Vehicle (UAV)-derived high-resolution topographic surveys significantly improves the quality and accuracy of topographic information required for highway geometric design. The comparison between the conventional GNSS survey and the integrated GNSS-UAV approach revealed notable differences in terrain representation, elevation modelling, point density, and overall survey quality, highlighting the advantages of combining both technologies for engineering applications (Colomina & Molina, 2014; Nex & Remondino, 2014).
The elevation comparison showed that both survey methods produced identical elevations at the control point (Chainage 0+000), confirming the reliability of the georeferencing process and the proper integration of the UAV survey with the GNSS control network. However, beyond the control point, the integrated GNSS-UAV survey generally produced slightly lower elevations than the GNSS-only survey, with elevation differences ranging from +0.265 m to −2.725 m. These differences indicate that the UAV-derived Digital Terrain Model (DTM) captured the actual ground surface more effectively by filtering vegetation, surface irregularities, and localized terrain variations that may not have been fully represented by the discrete GNSS observations. Similar observations have been reported by Nex & Remondino (2014), who noted that UAV photogrammetry provides a more detailed representation of complex terrain than conventional ground surveying techniques. Likewise, Turner, Lucieer, & Watson (2016) reported that UAV-derived terrain models improve the detection of subtle topographic features required for engineering design.
The Root Mean Square Error (RMSE) analysis further confirmed the consistency between both survey techniques. The calculated mean error of −1.366 m, RMSE of 1.463 m, and standard deviation of 0.526 m indicate that although systematic differences existed between the datasets, the variation remained relatively consistent throughout the study corridor. The predominance of negative errors suggests that the UAV-derived terrain model provided a more refined representation of the bare-earth surface than the conventional GNSS survey. Previous studies by James, Robson, d'Oleire-Oltmanns, & Niethammer, (2017); Agüera-Vega, Carvajal-Ramírez, & Martínez-Carricondo, (2017) similarly demonstrated that integrating UAV photogrammetry with

accurately established GNSS ground control points substantially improves vertical accuracy and reduces positional uncertainties in topographic mapping.

One of the most significant findings of this study is the enormous difference in survey point density. The conventional GNSS survey collected only 169 observation points, corresponding to a point density of 0.000166 points/m², whereas the integrated GNSS-UAV survey generated approximately 232.96 million points, representing 229.02 points/m². This dramatic increase in data density demonstrates the capability of UAV photogrammetry to capture continuous terrain information rather than isolated ground observations. High point density is particularly important in highway engineering because it enables accurate modelling of slopes, drainage channels, embankments, road shoulders, and other terrain features that influence highway alignment and construction. Similar improvements in terrain modelling using dense UAV point clouds have been reported by Colomina & Molina (2014) who concluded that UAV photogrammetry provides superior spatial detail compared with traditional surveying methods.

The UAV operational outputs further demonstrate the effectiveness of the integrated survey methodology. The successful acquisition of 3,162 aerial photographs, with 3,150 images successfully calibrated, representing a calibration success rate of approximately 99.6%, indicates excellent flight planning, adequate image overlap, and high-quality photogrammetric processing. Furthermore, the achieved Ground Sampling Distance (GSD) of 1.89 cm signifies an extremely high spatial resolution capable of capturing minute terrain details essential for engineering design. According to Eisenbeiss (2009), GSD values below 2 cm are considered highly suitable for engineering-grade topographic mapping and infrastructure projects requiring centimetre-level precision.

The Digital Terrain Model (DTM) generated from the three UAV survey blocks clearly illustrates the advantages of high-resolution terrain modelling. The seamless integration of the three blocks produced a continuous terrain surface capable of representing gradual elevation changes, slope transitions, embankments, and depressions across the study corridor. Unlike conventional GNSS surveys, which rely on interpolation between widely spaced points, the UAV-derived DTM directly measures the terrain surface using millions of observations. This finding agrees with the work of Westoby, Brasington, Glasser, Hambrey, & Reynolds, (2012), who emphasized that Structure-from-Motion (SfM) photogrammetry significantly enhances the representation of terrain morphology and surface continuity.

The comparison of terrain representation further supports the superiority of the integrated approach. Although both methods utilized the same 169 GNSS control points, the integration of UAV photogrammetry transformed these control points into a highly detailed three-dimensional terrain model through the generation of a dense point cloud. Consequently, the integrated approach achieved very high spatial resolution, excellent terrain detail, and direct surface representation, whereas the conventional GNSS survey provided only moderate terrain representation based on interpolated measurements. This enhanced surface characterization improves the reliability of highway alignment selection, earthwork estimation, drainage analysis, and slope stability assessment, all of which depend on accurate terrain information (Eltner, Kaiser, Castillo, Rock, Neugirg, & Abellán, (2016); James, Robson, d'Oleire-Oltmanns, & Niethammer, (2017).

Figures 2 and 3 present the Digital Terrain Models (DTMs) of Temboga 1 and Temboga 3, respectively, generated from the integrated GNSS-UAV survey. The two models collectively

demonstrate the capability of the integrated survey methodology to produce high-resolution three-dimensional representations of the terrain surface along different sections of the highway corridor. In both figures, the terrain surfaces are continuous and well-defined, indicating successful photogrammetric processing and accurate georeferencing using GNSS Ground Control Points, which are essential for achieving engineering-grade positional accuracy (James, Robson, d'Oleire-Oltmanns, & Niethammer, (2017); Agüera-Vega, Carvajal-Ramírez, & Martínez-Carricondo (2017).
The DTM of Temboga 1 reveals a corridor characterized by gradual elevation changes and localized terrain undulations, with the terrain rising from the lower southwestern section toward the northeastern end. The model clearly captures slope transitions, embankments, and subtle surface irregularities that would be difficult to represent adequately using conventional point-based GNSS surveys alone. Similarly, the DTM of Temboga 3 shows a generally ascending terrain profile, with elevation increasing progressively along the corridor. The colour gradient ranging from blue (lower elevations) through green (intermediate elevations) to yellow/orange (higher elevations) provides a clear visualization of the terrain morphology and slope variation, thereby enhancing terrain interpretation and engineering analysis (Westoby, Brasington, Glasser, Hambrey, & Reynolds, 2012).
The combined interpretation of both DTMs highlights the significant improvement in terrain representation achieved through the integrated GNSS-UAV approach. The dense point cloud generated from the UAV survey enabled the capture of fine-scale topographic features, including drainage paths, slope gradients, and potential cut-and-fill zones, which are critical for accurate longitudinal profile development, vertical curve design, earthwork estimation, and drainage planning (Colomina & Molina, 2014; Nex & Remondino, 2014). The integrated GNSS-UAV methodology demonstrated superior terrain characterization and enhanced engineering visualization, thereby improving the accuracy and reliability of highway design decisions for both Temboga 1 and Temboga 3 sections of the project corridor (Turner, Lucieer, & Watson, 2016); Eltner, Kaiser, Castillo, Rock, Neugirg, & Abellán, (2016).

Overall, the results clearly demonstrate that integrating GNSS with UAV photogrammetry substantially enhances highway topographic surveys by improving elevation modelling, increasing spatial resolution, and generating highly detailed terrain datasets. Although conventional GNSS surveying remains highly reliable for establishing horizontal and vertical control, its integration with UAV technology provides a more comprehensive representation of the terrain surface. These findings support the growing adoption of integrated geospatial technologies in modern highway engineering and agree with previous studies that advocate the combined use of GNSS and UAV systems to improve the accuracy, efficiency, and reliability of engineering surveys (Colomina & Molina, 2014; Nex & Remondino, 2014; Turner, Lucieer, & Watson, 2016); Agüera-Vega *et al.,* 2017). Consequently, the integrated GNSS-UAV survey approach offers a more robust foundation for highway geometric design, ultimately contributing to improved design accuracy, optimized earthwork calculations, reduced construction risks, and more sustainable transportation infrastructure development (Westoby, Brasington, Glasser, Hambrey, & Reynolds, 2012; James, Robson, d'Oleire-Oltmanns, & Niethammer, 2017).

4. CONCLUSION

This study demonstrated that the integration of Global Navigation Satellite System (GNSS) and Unmanned Aerial Vehicle (UAV)-derived high-resolution topographic surveys significantly enhances the accuracy and quality of topographic data required for highway geometric design. The comparative analysis revealed that although the conventional GNSS survey provided reliable positional control, the integration of UAV photogrammetry produced a much denser and more detailed representation of the terrain surface. Hence the findings of this study establish that integrating GNSS with UAV photogrammetry is superior to the use of conventional GNSS surveying alone for highway topographic surveys. The combined approach provides enhanced positional accuracy, substantially higher point density, better terrain representation, and greater operational efficiency. Therefore, the adoption of integrated GNSS-UAV surveying is recommended for modern highway engineering projects to improve design precision, reduce construction uncertainties, optimize project costs, and support the development of safe, efficient, and sustainable transportation infrastructure.

5. RECOMMENDATIONS

Adoption of integrated GNSS-UAV surveying: Highway agencies and engineering firms should adopt integrated GNSS-UAV surveying for highway planning, rehabilitation, and construction projects because it provides more accurate and detailed terrain information than conventional GNSS surveying alone. Use of adequate Ground Control Points (GCPs): A sufficient number of well-distributed GNSS Ground Control Points should be established in all UAV surveys to improve georeferencing accuracy and ensure engineering-grade terrain models. Application in highway rehabilitation projects: The integrated survey approach should be prioritized for highway rehabilitation projects where accurate identification of terrain undulations, drainage paths, and slope variations is essential for improving vertical alignment and reducing earthwork costs. Capacity building and training: Surveyors, geomatics engineers, and highway design professionals should receive regular training in UAV photogrammetry, GNSS data processing, and digital terrain modelling to enhance technical competence and encourage the adoption of modern geospatial technologies. Development of national guidelines: Government regulatory agencies should develop standardized guidelines and specifications for the use of UAV photogrammetry and integrated GNSS-UAV surveys in highway engineering projects to ensure data quality, consistency, and interoperability. Integration with GIS and BIM platforms: Future highway projects should integrate GNSS-UAV survey outputs with Geographic Information Systems (GIS) and Building Information Modelling (BIM) platforms to improve design coordination, visualization, and infrastructure management. Routine use for monitoring and maintenance: The integrated methodology should also be applied for post-construction monitoring, pavement deformation assessment, erosion mapping, and maintenance planning because UAV surveys allow rapid and cost-effective acquisition of up-to-date terrain information. Further research: Additional studies should evaluate the performance of integrated GNSS-UAV surveys in different terrain conditions, vegetation covers, and climatic environments, and compare the results with LiDAR-based surveys to establish the most suitable technology for various highway engineering applications.

REFERENCES

Agüera-Vega, F., Carvajal-Ramírez, F., & Martínez-Carricondo, P. (2017). Accuracy of digital surface models and orthophotos derived from unmanned aerial vehicle photogrammetry. *Journal of Surveying Engineering,* 143(2), 04016025. https://doi.org/10.1061/(ASCE)SU.1943-5428.0000206

Bang, K. I., Habib, A., Kim, E. M., & Kim, C. (2018). Integration of terrestrial laser scanning and UAV photogrammetry for highway corridor mapping. *Sensors, 18*(8), 2425.

Chiabrando, F., Nex, F., Piatti, D., & Rinaudo, F. (2011). UAV and RPV systems for photogrammetric surveys in archaeological areas: Two tests in the Piedmont region (Italy). *Journal of Archaeological Science, 38*(3), 697–710.

Colomina, I., & Molina, P. (2014). Unmanned aerial systems for photogrammetry and remote sensing: A review. ISPRS Journal of Photogrammetry and Remote Sensing, 92, 79–97. https://doi.org/10.1016/j.isprsjprs.2014.02.013

Eisenbeiss, H. (2009). *UAV photogrammetry*. ETH Zurich, Institute of Geodesy and Photogrammetry. Dissertation No. 18515.

Eltner, A., Kaiser, A., Castillo, C., Rock, G., Neugirg, F., & Abellán, A. (2016). Image-based surface reconstruction in geomorphometry—Merits, limits and developments. *Earth Surface Dynamics*, 4(2), 359–389. https://doi.org/10.5194/esurf-4-359-2016

Ghilani, C. D. (2018). *Adjustment Computations: Spatial Data Analysis* (6th ed.). Wiley.

James, M. R., Robson, S., d'Oleire-Oltmanns, S., & Niethammer, U. (2017). Optimising UAV topographic surveys processed with Structure-from-Motion: Ground control quality, quantity and bundle adjustment. Geomorphology, 280, 51–66. https://doi.org/10.1016/j.geomorph.2016.11.021

Luhmann, T., Robson, S., Kyle, S., & Harley, I. (2020). *Close-Range Photogrammetry and 3D Imaging* (3rd ed.). De Gruyter.

Nex, F., & Remondino, F. (2014). UAV for 3D mapping applications: A review. Applied Geomatics, 6(1), 1–15. https://doi.org/10.1007/s12518-013-0120-x

Turner, D., Lucieer, A., & Watson, C. (2016). An automated technique for generating georectified mosaics from ultra-high resolution unmanned aerial vehicle (UAV) imagery based on Structure-from-Motion point clouds. *Remote Sensing,* 4(5), 1392–1410. https://www.mdpi.com/2072-4292/4/5/1392

Westoby, M. J., Brasington, J., Glasser, N. F., Hambrey, M. J., & Reynolds, J. M. (2012). Structure-from-Motion photogrammetry: A low-cost, effective tool for geoscience applications. Geomorphology, 179, 300–314. https://doi.org/10.1016/j.geomorph.2012.08.021

Wolf, P. R., Ghilani, C. D., & Wilkinson, B. E. (2019). *Elementary Surveying: An Introduction to Geomatics* (15th ed.). Pearson.